

# Suppressing Uncertainties in Degradation Estimation for Blind Super-Resolution

Anonymous Authors

## ABSTRACT

The problem of blind image super-resolution aims to recover high-resolution (HR) images from low-resolution (LR) images with unknown degradation modes. Most existing methods model the image degradation process using blur kernels. However, this explicit modeling approach struggles to cover the complex and varied degradation processes encountered in the real world, such as high-order combinations of JPEG compression, blur, and noise. Implicit modeling for the degradation process can effectively overcome this issue, but a key challenge of implicit modeling is the lack of accurate ground truth labels for the degradation process to conduct supervised training. To overcome this limitations inherent in implicit modeling, we propose an Uncertainty-based degradation representation for blind Super-Resolution framework (USR). By suppressing the uncertainty of local degradation representations in images, USR facilitated self-supervised learning of degradation representations. The USR consists of two components: Adaptive Uncertainty-Aware Degradation Extraction (AUDE) and a feature extraction network composed of Variable Depth Dynamic Convolution (VDDC) blocks. To extract Uncertainty-based Degradation Representation from LR images, the AUDE utilizes the Self-supervised Uncertainty Contrast module with Uncertainty Suppression Loss to suppress the inherent model uncertainty of the Degradation Extractor. Furthermore, VDDC block integrates degradation information through dynamic convolution. Rhe VDDC also employs an Adaptive Intensity Scaling operation that adaptively adjusts the degradation representation according to the network hierarchy, thereby facilitating the effective integration of degradation information. Quantitative and qualitative experiments affirm the superiority of our approach.

## CCS CONCEPTS

• Computing methodologies → Image processing.

## KEYWORDS

Blind Super-Resolution, Learning with Uncertainty, Uncertainty-based Degradation Representation

## 1 INTRODUCTION

Image super-resolution (SR), a highly regarded task within the domain of low-level computer vision, seeks to reconstruct high-resolution (HR) images from their low-resolution (LR) counterparts

**Unpublished working draft. Not for distribution.**

Permission to make digital or hard copies of all or part of this work for personal or classroom use is granted by ACM, provided that the copies are not made for profit or commercial advantage and that copies bear this notice and the full citation on the first page. Copyrights for components of this work owned by others than the author(s) must be honored. Abstracting with credit is permitted. To copy otherwise, or republish, to post on servers or to redistribute to lists, requires prior specific permission and/or a fee. Request permissions from [permissions@acm.org](mailto:permissions@acm.org).

ACM MM, 2024, Melbourne, Australia

© 2024 Copyright held by the owner/author(s). Publication rights licensed to ACM.

ACM ISBN 978-x-xxxx-xxxx-x/YY/MM

<https://doi.org/10.1145/nnnnnnn.nnnnnn>

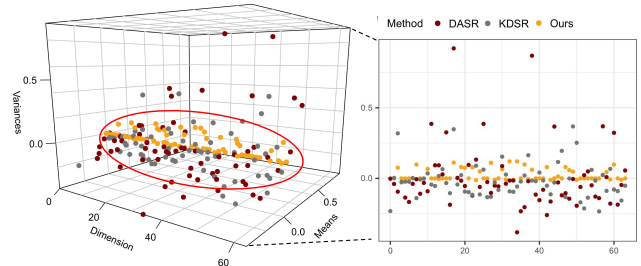


**Figure 1: Comparison on degradation estimation stability.** We randomly select different patches from the same image to compare the mean and variance of the degradation representations obtained by DASR, KDSR and USR. These methods exhibit varying degrees of instability, rooted in the inherent uncertainties of the model. USR (ours) demonstrates the most stable performance among them.

by augmenting the pixel count. This process involves deducing and restoring high-frequency details from a limited array of pixel information, thereby yielding images of enhanced clarity and detail. Conversely, image degradation represents the reverse procedure, wherein LR images are generated from their HR analogs. The degradation process is often unknown and complex, rendering the issue of blind super-resolution a formidable challenge. Modeling the image degradation process aids in reducing the complexity encountered by image SR models.

Traditional super-resolution techniques typically rely on interpolation methods [15, 43]. However, with the advent of deep learning, methods based on neural networks have significantly outpaced traditional approaches. These methods fall into two categories: model-based methods and learning-based methods. Model-based approaches simulate the image degradation process, estimating the degradation mode of LR images before reconstructing the HR images. These methods range from simple to complex, including those based on blur kernel estimation [13], spatially variant blur kernels [27, 66], and implicit modeling [21, 32, 47, 53] of the degradation process. They estimate the degradation mode for each LR image individually, hence are inclined to better generalize across unknown degradations. On the other hand, learning-based methods aim to train a unified super-resolution network using a vast corpus of LR/HR image pairs synthesized based on presumed degradation models [37, 64, 68]. Yet, these learning-based approaches are heavily dependent on the training data and may suffer significant performance drops when there is a domain discrepancy between the training and testing data [49]. Some efforts attempt to simulate real-world degradation patterns with more complex training samples, notable among which are BSRGAN [63] and Real-ESRGAN [48], employing advanced degradation models that incorporate blur, noise, resizing, and JPEG compression to generate training samples.

117 Researchers widely regard the challenge of addressing such complex  
118 degradation processes as blind super-resolution [42, 52, 53].

119 Model-based approaches predominantly rely on blur kernels.  
120 However, these methods possess limited representational capacity  
121 and can only cover blur-related degradation, falling short in the  
122 face of noise, JPEG compression, and other complex degradation  
123 processes. To address the nearly infinite degradation modes in  
124 blind super-resolution tasks, recent works have proposed using  
125 implicit modeling to characterize degradation patterns. DASR [47]  
126 employs contrastive learning to distance or draw closer feature  
127 representations of different degradation modes, whereas KDSR [53]  
128 uses knowledge distillation to enable a student network to learn  
129 the degradation representation from a teacher network.

130 As illustrated in Figure 1, DASR and KDSR exhibit instability in  
131 estimating degradation representations, meaning they fail to obtain  
132 consistent degradation representations for the same LR image. Such  
133 instability and inaccuracies in degradation representation adversely  
134 affect subsequent super-resolution processes. This instability is a  
135 manifestation of model uncertainty [11]. The root causes of the  
136 instability and unreliability in the degradation features of these  
137 methods are: (1) Due to the absence of ground truth, these methods  
138 provide only coarse constraints on the estimation process. (2) They  
139 overlook the uncertainty present in estimating implicit degradation  
140 representations, failing to offer confidence or uncertainty estimates  
141 for the generated outcomes.

142 To address this issue, we introduce an Uncertainty-based degrada-  
143 tion representation for blind Super-Resolution (USR) framework.  
144 To quantify and mitigate the uncertainty in Uncertainty-based  
145 Degradation Representation (UDR) estimation, we constrain UDR  
146 with Self-supervised Uncertainty Contrast which suppress the un-  
147 certainty of local degradation representations in images. Further-  
148 more, to ensure effective guidance of UDR, we have designed Vari-  
149 able Depth Dynamic Convolution (VDDC) Block. Thorough ex-  
150 perimentation validates the efficacy of our proposed modules. In  
151 summary, our contributions are as follows:

- 152 • We introduce the framework named **Uncertainty-based degrada-**  
153 **tion representation for blind Super-Resolution (USR)**. USR  
154 initially obtains Uncertainty-based Degradation Representation  
155 (UDR) from LR images through implicit modeling. To fully lever-  
156 age the UDR, we propose the Variable Depth Dynamic Convo-  
157 lution (VDDC) Block. With dynamic convolution and Adaptive  
158 Intensity Scaling (AIS) of UDR, VDDC effectively integrates im-  
159 age degradation information.
- 160 • We introduce the Adaptive Uncertainty-Aware Degradation Ex-  
161 traction (AUDE). Within AUDE, our proposed Self-supervised Un-  
162 certainty Contrast module employs USLoss to self-supervisedly  
163 constrain and mitigate the uncertainty inherent in the UDR esti-  
164 mation process. This approach not only addresses the challenge  
165 of implicit representations lacking true values but also enhances  
166 the model’s ability to adeptly handle various degradation modes.  
167 To our knowledge, we are the first to propose uncertainty mod-  
168 eling of the implicit representation for the image degradation  
169 process.
- 170 • Extensive experiments conducted on multiple representative  
171 datasets have demonstrated the performance of USR. A compre-  
172 hensive suite of qualitative experiments, quantitative analyses,

and ablation studies underscores the efficacy of our proposed  
175 modules. 176

## 177 2 RELATED WORK 178

### 179 2.1 Blind Super-Resolution 180

181 Contrary to the traditional Single Image Super-Resolution (SISR)  
182 task, the objective of blind super-resolution is to reconstruct HR  
183 images from their LR equivalents without prior knowledge of the  
184 degradation process [33, 44, 60]. Blind super-resolution methods  
185 can generally be categorized into the following two types.

186 **Model-based SR.** This category of SR models the image degrada-  
187 tion process. Most methods employ explicit modeling based on  
188 Equation (1), where  $k$  represents the blur kernel, and  $s$  denotes  
189 the downsampling factor. Within the realm of methods based on  
190 blur kernel estimation, IKC [13] introduced an iterative estima-  
191 tion technique and designed a correction function to accurately  
192 estimate the blur kernel or degradation features. Utilizing the prin-  
193 ciple of internal cross-scale recurrence, KernelGAN [5] interprets  
194 the maximization of patches within a single image as a problem  
195 of data distribution learning and trains a Generative Adversarial  
196 Network (GAN) across patches. MANet [27], a method based on  
197 the estimation of spatially variant blur kernels, estimates blur ker-  
198 nels with a network designed to have an optimally sized receptive  
199 field. However, these approaches struggle to address degradation  
200 modes beyond blur. In the domain of methods based on implicit  
201 degradation modeling, DASR[47] and KDSR [53] characterize the  
202 image degradation process using contrastive learning and knowl-  
203 edge distillation, respectively. However, due to the lack of effective  
204 constraints, DASR and KDSR are unstable and cannot fully extract  
205 discriminative degradation representations to guide blind super-  
206 resolution.

$$207 LR = (HR \otimes k) \downarrow_s + n \quad (1)$$

208 **Learning-based SR.** Learning-based methods endeavor to directly  
209 learn degradation patterns from training data in the form of high-  
210 level semantics, foregoing modeling the degradation process [28].  
211 SwinIR [26], by adopting the Swin Transformer for image restora-  
212 tion tasks, has achieved breakthrough performance. Works such  
213 as Restormer [61], HAT [8], and DAT [9] further demonstrate the  
214 potential of Vision Transformers in low-level visual tasks. Addition-  
215 ally, some researchers have focused on diffusion models [38, 45, 50,  
216 59], which transform complex and unstable generative processes  
217 into several independent and stable reverse processes through  
218 Markov chain modeling. However, due to the inherent random-  
219 ness of probabilistic models, images generated from the sampling  
220 space by diffusion models diverge from real images. Nonetheless,  
221 these efforts typically excel only within data distributions identical  
222 to their training sets, displaying limited generalizability.

### 223 2.2 Modeling Uncertainty for Super-Resolution 224

225 **Uncertainty in Deep Learning.** As deep learning continues to  
226 evolve, neural networks have permeated nearly every scientific  
227 domain, becoming integral to a myriad of real-world applications  
228 [10, 17, 20, 29, 57]. Researchers have devoted significant effort to  
229 understanding and quantifying the uncertainty in neural network  
230 predictions to enhance the performance and robustness of deep  
231

networks [35, 55, 58, 62]. In the field of computer vision, uncertainty modeling plays a pivotal role in critical tasks such as image classification [40, 46], object detection [16], semantic segmentation [4], face recognition [65, 67], action recognition [41, 62], and image generation [39]. The uncertainty in deep learning can broadly be categorized into two types: data uncertainty (also known as aleatoric uncertainty), which describes the intrinsic noise within the data, and model uncertainty (also known as epistemic uncertainty), which reflects the uncertainty inherent in the model itself due to inadequate training, insufficient training data, and other factors.

As shown on Equation (2), given a parameterized model  $f(\theta)$ , model uncertainty is formalized as a probability distribution over the model parameters  $\theta$ , while data uncertainty is formatted as a probability distribution over the model output  $y^*$ . The term  $p(\theta|D)$  is referred to as the posterior distribution of model parameters.  $D$  indicates the training dataset [11]. Our work focuses on model uncertainty within image degradation representation.

$$p(y^*|x^*, D) = \int \underbrace{p(y^*|x^*, \theta)}_{\text{Data}} \underbrace{p(\theta|D)}_{\text{Model}} d\theta \quad (2)$$

**Uncertainty-based SR.** To date, only a limited number of studies have explored the potential of uncertainty modeling in the task of super-resolution. SOSR [2] investigated the issue of source-free domain adaptation within super-resolution tasks through uncertainty modeling. DDL [30] utilized Bayesian methods to assess the reliability of high-frequency inference from a frequency domain perspective. [36] introduced an uncertainty-driven loss function that incorporates per-pixel uncertainty into super-resolution, giving priority to pixels with greater certainty, such as those representing texture and edges. Another study employed batch normalization uncertainty to analyze super-resolution uncertainty, thereby enhancing network robustness against adversarial attacks [22]. GRAM [25] focused neural network attention on challenging images through Gradient Rescaling Attention. However, none of these efforts addressed the blind super-resolution challenge associated with complex degradation processes.

## 3 METHOD

### 3.1 Overview

As previously mentioned, implicit modeling of complex and variable degradation processes represents a promising approach to addressing the issue of image blind super-resolution, with the lack of ground truth posing a significant challenge. To tackle this challenge, we employ an Uncertainty-based Degradation Representation (UDR) to model various degradation processes, adapting to complex and varied degradation scenarios.

As illustrated in Figure 2 (b), we implement Adaptive Uncertainty-Aware Degradation Extraction (AUDE) on LR images. In detail, we obtain the UDR from LR images using the Degradation Extractor (DE). To facilitate self-supervised training of UDR, we have devised the USLoss and a Self-supervised Uncertainty Contrast module. As depicted in Figure 2 (c), to effectively harness the information encapsulated within the UDR, we have designed a Variable Depth

Dynamic Convolution (VDDC) Block, which facilitates the modulation of UDR intensity in accordance with the depth of the network.

Overall, we utilize the DE to derive the UDR from LR images. Concurrently, the LR image undergoes initial shallow feature extraction via a convolutional layer, followed by deep feature extraction through  $N$  VDDCs.

### 3.2 Adaptive Uncertainty-Aware Degradation Extraction

Within AUDE, DE is tasked with extracting UDR from LR images. To suppress the uncertainty in the DE network, we employed USLoss within the Self-supervised Uncertainty Contrast to conduct self-supervised training of DE.

**Degradation Extractor.** Acknowledging the limitations of blur kernel modeling, which is confined to addressing solely blur-related degradation processes, we have adopted a more potent approach of implicit modeling for a comprehensive characterization of the degradation process. As depicted in Figure 2 (b), the DE extract degradation representations from LR images adaptively.

Initially, DE subjects the image to a preliminary feature extraction phase involving a  $3 \times 3$  convolutional layer followed by a ReLU layer. This is succeeded by the application of multiple convolutional blocks tasked with the extraction of deeper features. Each convolutional block is systematically composed of a  $3 \times 3$  convolutional layer, a ReLU layer, and another  $3 \times 3$  convolutional layer, arranged in sequence. The final stage of this process involves the refinement of the degradation representation vector through an average pooling layer and a Multilayer Perceptron (MLP).

Within the process of AUDE, during the training phase, two distinct patches are obtained from a LR image. The DE is employed to extract the corresponding UDR from these patches. By applying USLoss to suppress the uncertainty associated with these two UDRs, we guide the DE towards more stable degradation estimations. During inference, DE directly extracts a global UDR from the entire LR image.

**Self-supervised Uncertainty Contrast.** While different parts of the same image undergo nearly identical degradation, as illustrated in Figure 2 (b), the DE estimates significantly varied degradation representations from different patches of a LR image. This discrepancy reveals that without meticulous constraints, the UDR derived by DE is inconsistent and unstable, thus incapable of furnishing precise degradation information for subsequent SR networks. Ideally, however, the UDR obtained from different patches or the entire image should exhibit consistency. Our objective is for DE to estimate a unified and accurate degradation representation, both locally and globally. To address this challenge, we have designed a USLoss and a Self-supervised Uncertainty Contrast module to mitigate this uncertainty, enabling DE to estimate degradation representations more stably and accurately.

Let  $u_1$  and  $u_2$  represent the degradation representations obtained from two different patches  $x_1$  and  $x_2$  within a LR image. From probabilistic perspective, our training objective aims to maximize the joint distribution probability in Equation (3):

$$P(u_1|x_1; W, u_2|x_2; W) = P(u_1|x_1; W) \cdot P(u_2|x_2; W) \quad (3)$$

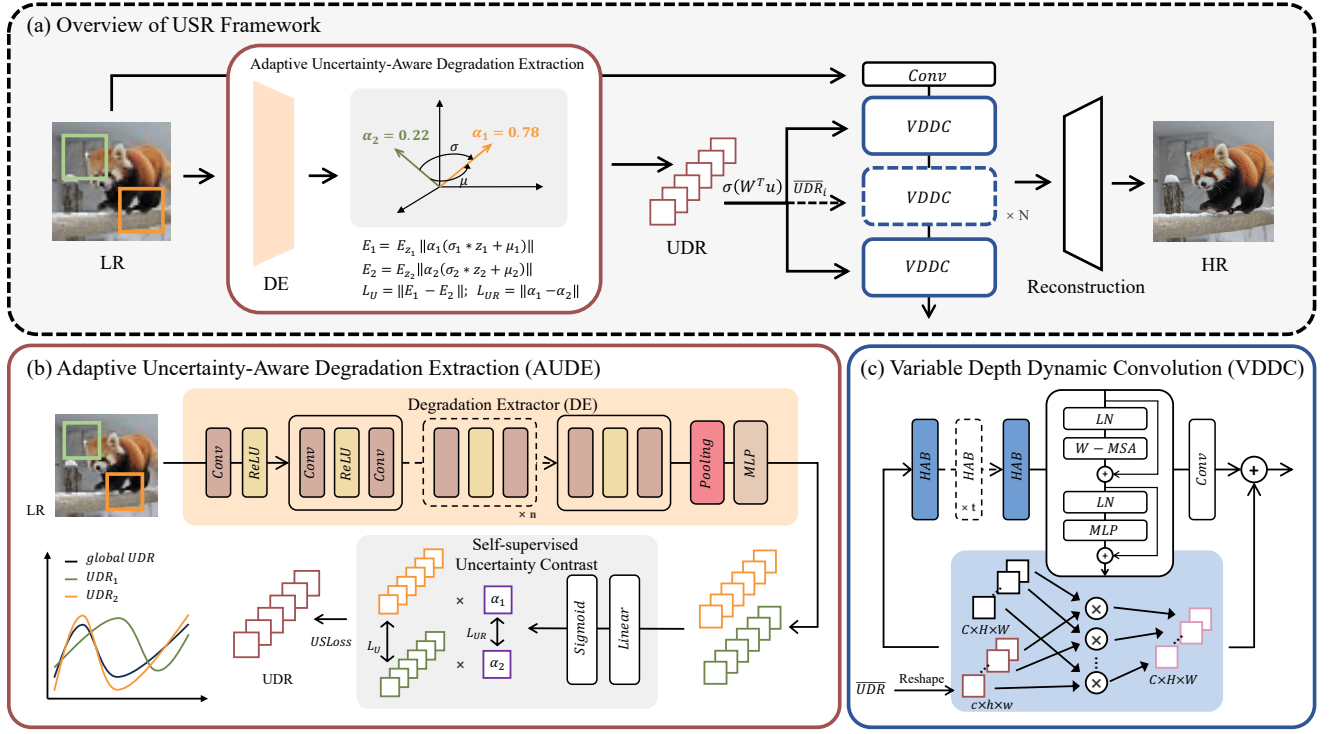


**Figure 2: The proposed framework Uncertainty-based degradation representation for blind Super-Resolution (USR).** (a) Illustration of the main process of USR. USR extracts Uncertainty-based Degradation Representation (UDR) from the LR image, which is then integrated with the super-resolution process through the VDDC. Reconstruction refers to the process of upsampling features. (b) Depiction of the Adaptive Uncertainty-Aware Degradation Extraction (AUDE). AUDE trains the Degradation Extractor (DE) in a self-supervised manner. (c) Depiction of the Variable Depth Dynamic Convolution (VDDC) Block. VDDC integrates UDR while extracting deep features from the LR image.

where  $W$  represents the parameters of the model. To maximize the aforementioned objective, we should aim to minimize the negative log likelihood of the joint distribution probability, where the random variables are  $u_1$  and  $u_2$ . Therefore, the optimization objective transforms into Equation (4):

$$E_{u_1, u_2 \sim P(u_1|x_1; W), P(u_2|x_2; W)} [P(u_1, u_2)] \quad (4)$$

To address this probability distribution, we model  $P(u|x; W)$  as a multivariate normal distribution, drawing upon the Central Limit Theorem (CLT) [24] and non-local means [7]. When there are sufficiently many random variables, their sum or average tends toward a normal distribution. This leads to Equation (5):

$$P(u|x; W) \sim N(\mu(x; W); \Sigma(x; W)) \quad (5)$$

The mean  $N$  and covariance  $\Sigma$ , outputs of the network parameterized by  $W$ , form the crux of our approach. However, the expectation in Equation (4) necessitates sampling  $u$  from  $P(u_1, u_2)$ , an operation intrinsically non-differentiable. To facilitate backpropagation through  $u$ , we employ reparameterization [23] to transfer the sampling process to the stochastic variable  $z \sim N(0, 1)$ , culminating in Equation (6):

$$E_{z_1, z_2 \sim N(0, 1)} [P(\mu_1 + \sigma_1 z_1 | \mu_2 + \sigma_2 z_2)] \quad (6)$$

In accordance with the conditional model delineated by the Gibbs distribution [6, 12], we arrive at Equation (7):

$$P(u_1, u_2) \propto \prod_i^{h \times w} \exp\left(-\frac{|u_1 - u_2|}{kT}\right) \quad (7)$$

The corresponding Gibbs energy is expressed in the form  $|u_1 - u_2|$ , with  $kT$  denoting the constant partition function [14]. Hence, we derive Equation (8):

$$\min_{E_{z_1, z_2}} \left[ \frac{1}{kT} \sum_i^{h \times w} |(\mu_{i1} - \mu_{i2}) + (\sigma_{i1} z_1 - \sigma_{i2} z_2)| \right] \quad (8)$$

Equation (8) impartially treats patches from different regions of an image. However, due to the inherent model uncertainty present in the feature extraction process of DE, the degradation representations extracted from different patches are not stable [10, 11, 48]. Aiming to direct DE towards a representation of degradation with diminished uncertainty, we have conceptualized the Self-supervised Uncertainty Contrast module. Within this module, a sequence of a linear layer and a Sigmoid layer is employed to deduce a learnable

variable, the Uncertainty Aware weight  $\alpha$ . This weight is then multiplied by the degradation representation to adaptively modulate its expressive intensity. Furthermore, we refine Equation (8), orienting it towards a suppression of the uncertainty estimated by DE in the direction of lower uncertainty, yielding Equation (9):

$$L_U = E_{z_1, z_2} \left[ \frac{1}{kT} \sum_i^{h \times w} |\alpha_1 (\mu_{i1} + \sigma_{i1} z_1) - \alpha_2 (\mu_{i2} + \sigma_{i2} z_2)| \right] \quad (9)$$

To prevent the DE from degrading to a local optimum during the training process, we incorporate a regularization term based on the Uncertainty Aware weight  $\alpha$ . This compels the Self-supervised Uncertainty Contrast module to discriminate the uncertainty among different patches, as indicated in Equation (10):

$$L_{UR} = |\alpha_1 - \alpha_2| \quad (10)$$

In summary, the final USLoss is encapsulated in Equation (11), where  $\lambda$  represents scaling weight.

$$USLoss = L_U - \lambda L_{UR} \quad (11)$$

Through Equation (11), we have mitigated the uncertainty inherent in the DE estimation process of degradation representation, which we term as Uncertainty-based Degradation Representation (UDR).

### 3.3 Variable Depth Dynamic Convolution Block

Through uncertainty modeling, we acquire the UDR via the Degradation Extractor (DE). To leverage UDR to its fullest extent, we have crafted the Variable Depth Dynamic Convolution (VDDC) Block, which adjusts the intensity of UDR based on the depth of the network and efficiently mines the feature information of images.

In the feature extraction segment, we adopt the design from HAB [8], wherein the channel attention within HAB and the design of the window-based multi-head self-attention [31] have been proven to effectively extract features. Each VDDC, in addition to  $t$  HABs, also includes a residual group composed of a layer normalization, a W-MSA layer [31], another layer normalization and an MLP, as well as a  $3 \times 3$  convolutional layer for fine-tuning the features.

As illustrated in Figure 2 (c) and inspired by KDSR [53] and UDVD [54], we integrate UDR using dynamic convolution. We first reshape UDR to the dimensions of  $c \times h \times w$ , and let  $F$  denote a feature map with dimensions  $C \times H \times W$ . For each channel  $i$ , the convolution output  $O_i$  at position  $(x, y)$  can be described by Equation (12).

$$O_i(x, y) = \sum_{m=0}^h \sum_{n=0}^w F_i(x+m, y+n) \cdot u_i(m, n) \quad (12)$$

where  $u$  represents the dynamic convolution weights, and  $O$  denotes the output features with dimensions  $C \times H \times W$ . However, in such a feature fusion approach, the UDR introduced at different depths of the network remains constant. A more rational approach would involve adaptively adjusting the intensity of the UDR input based on the network hierarchy. Thus, inspired by the concept of [46], we perform an Adaptive Intensity Scaling operation (AIS) on UDR before the dynamic convolution, as illustrated in Equation (13).

$$\overline{UDR}_i = \gamma_i \times UDR \quad (13)$$

The adaptive scaling parameter  $\gamma$  is derived as Equation (14).

$$\gamma_i = \sigma_i (W^T u + b) \quad (14)$$

where  $\sigma$  refers to activation function,  $W$  represents the transformation matrix and  $b$  represents the linear bias.

## 4 EXPERIMENT

### 4.1 Experiment Setup

**Implementation details.** In the DE, the number of convolutional blocks is set to 5; the MLP consists of three linear layers and three LeakyReLU layers in alternation. The scaling weight  $\lambda$  in USLoss is set to 0.1. USR incorporates 7 VDDC blocks, each containing 6 HABs. For the activation function in Equation (14), we have chosen the Sigmoid. The MLP within the VDDC adheres to the configuration specified in [31]. The final Reconstruction segment comprises a convolutional layer, a pixel shuffle layer, and another convolutional layer to upsample the feature map into an image.

USR is trained on a mixed dataset comprising DIV2K and Flickr2K. The training process is divided into three stages: (1) We train the VDDC to extract image features using MSE Loss; (2) Subsequently, by leveraging USLoss to suppress model uncertainty, we undertake self-supervised training of the DE; (3) Finally, the network is fine-tuned using L1 Loss. More Implementation details will be offered in the **supplementary materials**.

**Testing datasets.** We conducted comparisons between USR and several representative methods across six widely used datasets: DIV2K [1], BSDS [3], Urban100 [18], T91 [56], DPED [19] and DRealSR [51]. Synthetic data were generated following the workflow proposed by Real-ESRGAN [48].

### 4.2 Comparison With Existing Methods

**Compared Methods.** To evaluate the effectiveness and performance of our method, we compared USR with current state-of-the-art and representative blind super-resolution approaches, including DAN [34], DCLS [33], DASR [47], MANet [27], KDSR [53], SwinIR [26], HAT [8], Real-ESRGAN [48], and ResShift [59]. We tested these methods using their officially available codes.

**Quantitative Comparisons.** Quantitative results from the Table 1 reveal USR's significant advantages across multiple datasets, particularly in the image super-resolution domain. At a  $\times 4$  magnification factor, USR achieved the highest PSNR and SSIM on nearly all datasets.

On the DIV2K validation set, USR reached a PSNR of 23.96 dB, surpassing other methods, and led in SSIM with a score of 0.78, demonstrating its exceptional capability in restoring high-quality images. Similarly, on the BSDS100 and Urban100 datasets, USR not only led in PSNR with scores of 29.89 dB and 22.53 dB, respectively, but also achieved the highest SSIM scores of 0.92 and 0.77, further proving its robust performance across different types of images.

Notably, on the DRealSR dataset, even when facing complex real-world scenes, USR maintained a high level of performance with a PSNR of 31.02 dB, slightly higher than other methods. This result is particularly significant considering the test's closer alignment with

523  
524  
525  
526  
527  
528  
529  
530  
531  
532  
533  
534  
535  
536  
537  
538  
539  
540  
541  
542  
543  
544  
545  
546  
547  
548  
549  
550  
551  
552  
553  
554  
555  
556  
557  
558  
559  
560  
561  
562  
563  
564  
565  
566  
567  
568  
569  
570  
571  
572  
573  
574  
575  
576  
577  
578  
579  
580

**Table 1: Quantitive results on DIV2K, BSDS100, Urban100, T91, DPED and DRealSR datasets for scaling factor  $\times 4$ . Bold indicates the best performance.**

Datasets	Method	DAN	DCLS	DASR	MANet	KDSR	SwinIR	HAT	RealESRGAN	ResShift	USR (Ours)
		DIV2K [1]	PSNR	22.17	22.41	21.45	18.95	22.79	22.08	22.01	22.23
	SSIM	0.72	0.74	0.67	0.60	0.75	0.73	0.72	0.73	0.72	<b>0.78</b>
BSDS100 [3]	PSNR	27.95	28.03	28.79	22.79	27.50	26.08	28.04	26.62	26.40	<b>29.89</b>
	SSIM	0.87	0.89	0.89	0.77	0.88	0.84	0.87	0.85	0.81	<b>0.92</b>
Urban100 [18]	PSNR	20.26	21.18	21.36	17.05	21.28	20.37	19.56	20.61	21.71	<b>22.53</b>
	SSIM	0.69	0.72	0.73	0.54	0.74	0.71	0.67	0.72	0.74	<b>0.77</b>
T91 [56]	PSNR	33.14	<b>33.82</b>	33.64	27.24	30.30	29.41	33.49	29.82	27.93	31.21
	SSIM	0.93	0.93	0.94	0.90	0.94	0.92	0.93	0.93	0.85	<b>0.95</b>
DPED-blackberry [19]	PSNR	22.96	23.38	23.54	20.22	22.92	22.04	22.75	21.89	22.49	<b>24.20</b>
	SSIM	0.74	0.76	0.76	0.64	0.75	0.72	0.74	0.72	0.71	<b>0.78</b>
DPED-iphone [19]	PSNR	25.52	26.05	26.00	21.08	24.88	23.79	25.43	23.71	24.37	<b>26.77</b>
	SSIM	0.82	0.84	0.84	0.71	0.82	0.80	0.82	0.79	0.79	<b>0.86</b>
DPED-sony [19]	PSNR	20.43	20.90	21.02	18.95	20.98	20.72	20.20	20.56	20.86	<b>23.92</b>
	SSIM	0.64	0.66	0.66	0.57	0.66	0.65	0.64	0.65	0.63	<b>0.69</b>
DRealSR [51]	PSNR	31.00	30.97	30.98	27.42	29.89	28.45	30.96	29.94	25.77	<b>31.02</b>
	SSIM	0.92	0.92	0.92	0.90	0.91	0.89	<b>0.93</b>	0.92	0.71	0.91

real-world applications. Although slightly below the highest SSIM score, USR’s performance remains impressive given the complexity of real scenarios.

Overall, USR’s consistently high performance across various datasets highlights its remarkable advantages in the field of image super-resolution, especially in handling real-world images. Comparing different methods shows that USR excels not only in traditional evaluation standards but also in adapting to and managing complex real-world scenes.

**Qualitative Comparisons.** As illustrated in Figure 3, due to the inherent challenges of the blind super-resolution task, super-resolution models encounter issues such as distortion and artifacts. Compared to other methods, USR excels in preserving the authenticity of the original image and restoring details. Observing the HR image alongside the image processed by USR, one can clearly see USR’s significant advantage in maintaining the overall structure and color fidelity of the image.

In the case of stained glass, USR not only faithfully preserves the color and sheen of the glass but also demonstrates superior clarity in edges and details compared to other methods. Particularly in the intricate depiction of the stained glass’s central pattern, USR reveals detail levels and color gradients close to the original, whereas other methods exhibit some distortion in these aspects.

In urban street scene case, USR similarly showcases its strengths. Observing the window frames and the brickwork on walls, USR’s precision in detail restoration is evident. In contrast, other methods are either too blurry, losing some details, or too sharp, resulting in unnatural artifacts along edges. USR achieves a good balance in handling these details, restoring true textures and depth, making the image closer to the original high-resolution version.

In summary, USR not only provides a more natural and smooth overall visual experience but also maintains a high fidelity in restoring everything from subtle textures to macro structures. Its performance surpasses other super-resolution methods in several aspects, whether it’s in detail sharpening, color accuracy, or the naturalness in avoiding over-processing. More Qualitative comparison results will be offered in the **supplementary materials**.

### 4.3 Ablation Study

**Effectiveness of AUDE and AIS.** As shown in Table 2, we conducted experiments across multiple datasets to validate the effectiveness of AUDE and AIS. AUDE is a crucial component of USR, achieving the implicit representation of the image degradation process; AIS is a vital element of VDDC, performing adaptive intensity adjustments to UDR based on the network hierarchy.

Evaluation results on three distinct datasets—DIV2K, BSDS100, and Urban100—demonstrate that the simultaneous application of AUDE and AIS yields the highest PSNR and SSIM scores. Notably, on the DIV2K dataset, PSNR and SSIM reached 23.96 and 0.78, respectively; on the BSDS100 dataset, scores were 29.89 and 0.92, respectively; and on the Urban100 dataset, the scores were 22.53 and 0.77. This starkly contrasts with results obtained using AUDE or AIS alone, where the performance with just AUDE outperforms that with only AIS.

As shown in Table 3, we also analyzed the performance with different numbers of VDDC blocks  $N$ . The findings reveal that an optimal performance is achieved with 7 VDDC blocks (our approach), manifesting in a PSNR of 23.96 and a SSIM of 0.78 on DIV2K; a PSNR of 29.89 and a SSIM of 0.91 on BSDS100; and a PSNR of 22.53

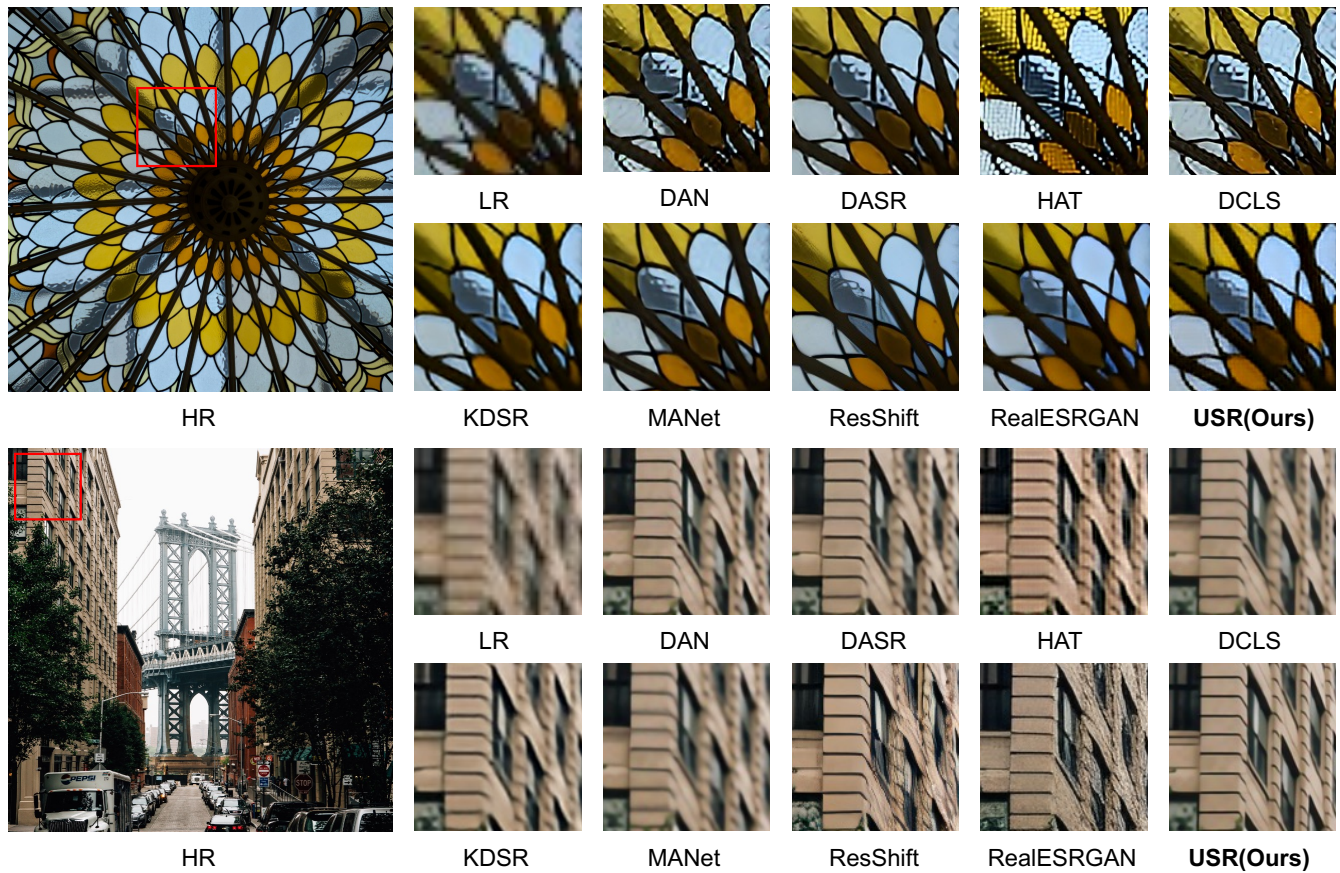


Figure 3: Visual comparisons of several representative methods on examples of the DIV2K dataset. The image above is a case of stained glass, while the image below depicts a urban street scene.

Table 2: Ablation study on the proposed Adaptive Uncertainty-Aware Degradation Extraction (AUDE) and Adaptive Intensity Scaling (AIS).

AUDE	AIS	DIV2K		BSDS100		Urban100	
		PSNR	SSIM	PSNR	SSIM	PSNR	SSIM
✓	✗	22.85	0.67	28.71	0.82	21.55	0.67
✗	✓	16.88	0.52	19.35	0.64	16.69	0.51
✓	✓	<b>23.96</b>	<b>0.78</b>	<b>29.89</b>	<b>0.92</b>	<b>22.53</b>	<b>0.77</b>

and SSIM of 0.77 on Urban100. In contrast, configurations featuring alternative quantities of VDDC blocks experience a marginal decline in performance.

**Effectiveness of USLoss.** Figure 4 presents ablation experiments on USLoss. From left to right, the images display the LR image, HR image, and the results processed by USR under three different configurations. In Figure 4 (a), the reconstructed image exhibits noticeable color distortions in certain areas, particularly in the diagonal sections of the image, where purple and blue spots and stripes are visible, significantly differing from the original high-resolution image’s tones. This distortion likely results from the

Table 3: Performance on DIV2K, BSDS100 and Urban100 datasets for different VDDC number  $N$ .

Number of VDDC	DIV2K		BSDS100		Urban100	
	PSNR	SSIM	PSNR	SSIM	PSNR	SSIM
6	23.20	0.76	28.66	0.90	21.66	0.73
7 (Ours)	<b>23.96</b>	<b>0.78</b>	<b>29.89</b>	<b>0.91</b>	<b>22.53</b>	<b>0.77</b>
8	23.22	0.76	28.68	0.89	21.71	0.73
10	23.65	0.77	29.31	0.90	22.18	0.76

loss function’s lack of constraints on model estimation uncertainty. In Figure 4 (b), beyond color distortion, there are also structural distortions and geometric distortions in the image. Observing the seams of diagonals and wall corners, it is apparent that lines have been inaccurately reconstructed, leading to bending and twisting, contrasting with the original image’s straight lines and sharp edges. These structural distortions indicate that without  $L_{UR}$ , USR falls short in maintaining image geometric integrity and edge clarity. Lastly, Figure 4 (c) showcases the USR method employing both  $L_U$  and  $L_{UR}$  (our method), where, in this scenario, PSNR significantly increases to 22.11, and SSIM to 0.86. This demonstrates that the

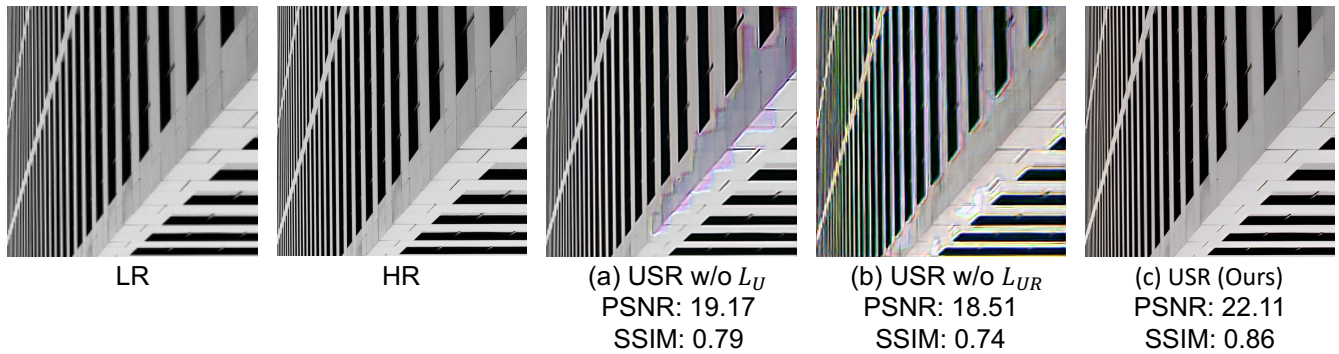


**Figure 4: Visualization of ablation study on USLoss.**  $L_U$  and  $L_{UR}$  represent the two components of USLoss. (a) represents USR trained without  $L_U$ ; (b) depicts USR trained without  $L_{UR}$ ; (c) shows USR trained with USLoss.

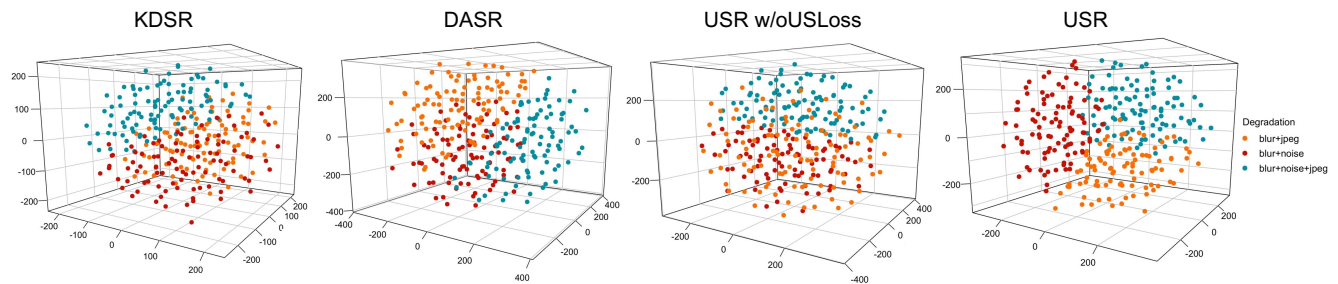


**Figure 5: The t-SNE visualizations on the DIV2K datasets.** Blur, noise, and JPEG compression represent common degradation modes in real-world scenarios. We conducted cluster analysis experiments under their various combinations. USR (Ours) effectively distinguishes between different degradation modes.

USR method, incorporating both types of loss functions, can better restore image details, closely matching the HR image.

**t-SNE visualization of degradation representation.** Figure 5 uses the t-SNE visualization to demonstrate how four SR algorithms manage various image degradations, with each dot color denoting a different degradation cluster. USR’s plot shows tightly clustered points for each degradation mode, highlighting its effective differentiation, while USR without USLoss shows dispersed clusters, underscoring USLoss’s importance. KDSR exhibits moderate clustering, less distinct than USR, and DASR shows the most scattered distribution, indicating its lower effectiveness with mixed degradations. These results underscore USLoss’s crucial role in improving SR algorithms’ ability to discern between degradation modes.

**Comparison on various degradation modes.** As shown in Table 4, experiments conducting quantitative comparisons across various degradation modes on the DIV2K dataset demonstrate the exceptional generalization capability of the USR algorithm. USR achieved the highest PSNR and SSIM values across all considered combinations of degradation modes (blur+noise+JPEG, blur+noise, blur+JPEG). Notably, in the composite degradation scenario of blur, noise, and JPEG compression, USR led with a PSNR of 23.96 and an SSIM of 0.78, significantly outperforming other methods. This underscores USR’s outstanding adaptability and robustness in handling multiple degradation effects, effectively enhancing image

quality and maintaining high performance even amidst complex interwoven degradation modes.

**Table 4: Quantitative comparison of different methods under various degradation modes on the DIV2K dataset.**

Method	blur+noise+JPEG		blur+noise		blur+JPEG	
	PSNR	SSIM	PSNR	SSIM	PSNR	SSIM
DASR	21.45	0.67	23.04	0.75	23.07	0.75
KDSR	22.79	0.75	22.79	0.75	22.78	0.75
USR	<b>23.96</b>	<b>0.78</b>	<b>23.19</b>	<b>0.76</b>	<b>23.24</b>	<b>0.76</b>

## 5 CONCLUSION

In summary, our proposed Uncertainty-based Super-Resolution (USR) framework effectively addresses the challenge of blind image super-resolution by leveraging implicit modeling. Through Adaptive Uncertainty-Aware Degradation Extraction (AUDE) and the Self-supervised Uncertainty Contrast module, USR accurately extracts degradation information and facilitates self-supervised training. In future work, we aim to further investigate how to address the complex and varied degradation processes in image super-resolution tasks through more refined modeling approaches. Additionally, we aspire to delve deeper into the potential of uncertainty learning within low-level vision tasks.

## REFERENCES

- [1] Eirikur Agustsson and Radu Timofte. 2017. NTIRE 2017 Challenge on Single Image Super-Resolution: Dataset and Study. In *The IEEE Conference on Computer Vision and Pattern Recognition (CVPR) Workshops*.
- [2] Yuang Ai, Xiaoqiang Zhou, Huaibo Huang, Lei Zhang, and Ran He. 2023. SOSR: Source-free image super-resolution with wavelet augmentation transformer. *arXiv preprint arXiv:2303.17783* (2023).
- [3] Pablo Arbelaez, Michael Maire, Charless Fowlkes, and Jitendra Malik. 2011. Contour Detection and Hierarchical Image Segmentation. *IEEE Trans. Pattern Anal. Mach. Intell.* 33, 5 (May 2011), 898–916. <https://doi.org/10.1109/TPAMI.2010.161>
- [4] Vijay Badrinarayanan, Alex Kendall, and Roberto Cipolla. 2017. SegNet: A Deep Convolutional Encoder-Decoder Architecture for Image Segmentation. *IEEE Transactions on Pattern Analysis and Machine Intelligence* (Dec 2017), 2481–2495. <https://doi.org/10.1109/tpami.2016.2644615>
- [5] Sefi Bell-Kligler, Assaf Shocher, and Michal Irani. 2019. Blind super-resolution kernel estimation using an internal-gan. *Advances in Neural Information Processing Systems* 32 (2019).
- [6] Joan Bruna, Pablo Sprechmann, and Yann LeCun. 2016. Super-Resolution with Deep Convolutional Sufficient Statistics. *International Conference on Learning Representations, International Conference on Learning Representations* (Jan 2016).
- [7] A. Buades, B. Coll, and J.-M. Morel. 2005. A Non-Local Algorithm for Image Denoising. In *2005 IEEE Computer Society Conference on Computer Vision and Pattern Recognition (CVPR'05)*. <https://doi.org/10.1109/cvpr.2005.38>
- [8] Xiangyu Chen, Xintao Wang, Jiantao Zhou, Yu Qiao, and Chao Dong. 2023. Activating More Pixels in Image Super-Resolution Transformer. In *Proceedings of the IEEE/CVF Conference on Computer Vision and Pattern Recognition (CVPR)*. 22367–22377.
- [9] Zheng Chen, Yulun Zhang, Jinjin Gu, Linghe Kong, Xiaokang Yang, and Fisher Yu. 2023. Dual Aggregation Transformer for Image Super-Resolution. In *ICCV*.
- [10] Yarín Gal and Zoubin Ghahramani. 2015. Dropout as a Bayesian Approximation: Representing Model Uncertainty in Deep Learning. *Cornell University - arXiv, Cornell University - arXiv* (Jun 2015).
- [11] Jakob Gawlikowski, Cedricque Rovile Njéutcheu Tassi, Mohsin Ali, Jongseok Lee, Matthias Humt, Jianxiang Feng, Anna Kruspe, Rudolph Triebel, Peter Jung, Ribana Roscher, et al. 2023. A survey of uncertainty in deep neural networks. *Artificial Intelligence Review* 56, Suppl 1 (2023), 1513–1589.
- [12] Stuart Geman and Donald Geman. 1984. Stochastic relaxation, Gibbs distributions, and the Bayesian restoration of images. *IEEE Transactions on pattern analysis and machine intelligence* 6 (1984), 721–741.
- [13] Jinjin Gu, Hannan Lu, Wangmeng Zuo, and Chao Dong. 2019. Blind super-resolution with iterative kernel correction. In *The IEEE Conference on Computer Vision and Pattern Recognition (CVPR)*.
- [14] Xiangyu He and Jian Cheng. 2022. Revisiting L1 loss in super-resolution: a probabilistic view and beyond. *arXiv preprint arXiv:2201.10084* (2022).
- [15] Hsieh Hou and H. Andrews. 1978. Cubic splines for image interpolation and digital filtering. *IEEE Transactions on Acoustics, Speech, and Signal Processing* 26, 6 (Dec 1978), 508–517. <https://doi.org/10.1109/tassp.1978.1163154>
- [16] Chao Huang, Chengliang Liu, Zheng Zhang, Zhihao Wu, Jie Wen, Qiuping Jiang, and Yong Xu. 2022. Pixel-Level Anomaly Detection via Uncertainty-aware Prototypical Transformer. In *MM '22: The 30th ACM International Conference on Multimedia, Lisboa, Portugal, October 10 - 14, 2022*, João Magalhães, Alberto Del Bimbo, Shin'ichi Satoh, Nicu Sebe, Xavier Alameda-Pineda, Qin Jin, Vincent Oria, and Laura Toni (Eds.). ACM, 521–530. <https://doi.org/10.1145/3503161.3548082>
- [17] Huimin Huang, Yawen Huang, Shiao Xie, Lanfen Lin, Ruofeng Tong, Yen-Wei Chen, Yuexiang Li, and Yefeng Zheng. 2023. Semi-Supervised Convolutional Vision Transformer with Bi-Level Uncertainty Estimation for Medical Image Segmentation. In *Proceedings of the 31st ACM International Conference on Multimedia, MM 2023, Ottawa, ON, Canada, 29 October 2023- 3 November 2023*, Abdumotaleb El-Saddik, Tao Mei, Rita Cucchiara, Marco Bertini, Diana Patricia Tobon Vallejo, Pradeep K. Atrey, and M. Shamim Hossain (Eds.). ACM, 5214–5222. <https://doi.org/10.1145/3581783.3611821>
- [18] Jia-Bin Huang, Abhishek Singh, and Narendra Ahuja. 2015. Single Image Super-Resolution From Transformed Self-Exemplars. In *Proceedings of the IEEE Conference on Computer Vision and Pattern Recognition*. 5197–5206.
- [19] Andrey Ignatov, Nikolay Kobyshev, Radu Timofte, Kenneth Vanhoey, and Luc Van Gool. 2017. DSLR-Quality Photos on Mobile Devices with Deep Convolutional Networks. In *Proceedings of the IEEE International Conference on Computer Vision*. 3277–3285.
- [20] Runhua Jiang and Yahong Han. 2023. Uncertainty-Aware Variate Decomposition for Self-supervised Blind Image Deblurring. In *Proceedings of the 31st ACM International Conference on Multimedia, MM 2023, Ottawa, ON, Canada, 29 October 2023- 3 November 2023*, Abdumotaleb El-Saddik, Tao Mei, Rita Cucchiara, Marco Bertini, Diana Patricia Tobon Vallejo, Pradeep K. Atrey, and M. Shamim Hossain (Eds.). ACM, 252–260. <https://doi.org/10.1145/3581783.3612535>
- [21] Shuo Jin, Meiqin Liu, Chao Yao, Chunyu Lin, and Yao Zhao. 2023. Kernel Dimension Matters: To Activate Available Kernels for Real-time Video Super-Resolution. In *Proceedings of the 31st ACM International Conference on Multimedia, MM 2023, Ottawa, ON, Canada, 29 October 2023- 3 November 2023*, Abdumotaleb El-Saddik, Tao Mei, Rita Cucchiara, Marco Bertini, Diana Patricia Tobon Vallejo, Pradeep K. Atrey, and M. Shamim Hossain (Eds.). ACM, 8617–8625. <https://doi.org/10.1145/3581783.3611908>
- [22] Aupendu Kar and Prabir Kumar Biswas. 2019. Fast Bayesian Uncertainty Estimation of Batch Normalized Single Image Super-Resolution Network. *arXiv: Computer Vision and Pattern Recognition, arXiv: Computer Vision and Pattern Recognition* (Mar 2019).
- [23] Diederik P. Kingma and Max Welling. 2013. Auto-Encoding Variational Bayes. *arXiv: Machine Learning, arXiv: Machine Learning* (Dec 2013).
- [24] Sang Gyu Kwak and Jong Hae Kim. 2017. Central limit theorem: the cornerstone of modern statistics. *Korean journal of anesthesiology* 70, 2 (2017), 144.
- [25] Chang-Woo Lee and Chung Ki-Seok. 2019. GRAM: Gradient Rescaling Attention Model for Data Uncertainty Estimation in Single Image Super Resolution. *IEEE Conference Proceedings, IEEE Conference Proceedings* (Jan 2019).
- [26] Jingyun Liang, Jiezhang Cao, Guolei Sun, Kai Zhang, Luc Van Gool, and Radu Timofte. 2021. SwinIR: Image Restoration Using Swin Transformer. *arXiv preprint arXiv:2108.10257* (2021).
- [27] Jingyun Liang, Guolei Sun, Kai Zhang, Luc Van Gool, and Radu Timofte. 2021. Mutual Affine Network for Spatially Variant Kernel Estimation in Blind Image Super-Resolution. In *IEEE International Conference on Computer Vision*.
- [28] Bee Lim, Sanghyun Son, Heewon Kim, Seungjun Nah, and Kyoung Mu Lee. 2017. Enhanced Deep Residual Networks for Single Image Super-Resolution. In *The IEEE Conference on Computer Vision and Pattern Recognition (CVPR) Workshops*.
- [29] Hanwei Liu, Huiling Cai, Qingcheng Lin, Xuefeng Li, and Hui Xiao. 2023. Learning from More: Combating Uncertainty Cross-multidomain for Facial Expression Recognition. In *Proceedings of the 31st ACM International Conference on Multimedia, MM 2023, Ottawa, ON, Canada, 29 October 2023- 3 November 2023*, Abdumotaleb El-Saddik, Tao Mei, Rita Cucchiara, Marco Bertini, Diana Patricia Tobon Vallejo, Pradeep K. Atrey, and M. Shamim Hossain (Eds.). ACM, 5889–5898. <https://doi.org/10.1145/3581783.3611702>
- [30] Tao Liu, Jun Cheng, and Shan Tan. 2023. Spectral Bayesian uncertainty for image super-resolution. In *Proceedings of the IEEE/CVF Conference on Computer Vision and Pattern Recognition*. 18166–18175.
- [31] Ze Liu, Yutong Lin, Yue Cao, Han Hu, Yixuan Wei, Zheng Zhang, Stephen Lin, and Baining Guo. 2021. Swin transformer: Hierarchical vision transformer using shifted windows. In *Proceedings of the IEEE/CVF international conference on computer vision*. 10012–10022.
- [32] Xiaotong Luo, Yuan Xie, Yulun Zhang, Yanyun Qu, Cuihua Li, and Yun Fu. 2020. Latticenet: Towards lightweight image super-resolution with lattice block. In *Computer Vision—ECCV 2020: 16th European Conference, Glasgow, UK, August 23–28, 2020, Proceedings, Part XXII* 16. Springer, 272–289.
- [33] Ziwei Luo, Haibin Huang, Lei Yu, Youwei Li, Haoqiang Fan, and Shuaicheng Liu. 2022. Deep constrained least squares for blind image super-resolution. In *Proceedings of the IEEE/CVF Conference on Computer Vision and Pattern Recognition*. 17642–17652.
- [34] Zhengxiong Luo, Yan Huang, Shang Li, Liang Wang, and Tieniu Tan. 2020. Unfolding the Alternating Optimization for Blind Super Resolution. *Advances in Neural Information Processing Systems (NeurIPS)* 33 (2020).
- [35] Yanbiao Ma, Licheng Jiao, Fang Liu, Shuyuan Yang, Xu Liu, and Lingling Li. 2023. Orthogonal Uncertainty Representation of Data Manifold for Robust Long-Tailed Learning. In *Proceedings of the 31st ACM International Conference on Multimedia, MM 2023, Ottawa, ON, Canada, 29 October 2023- 3 November 2023*, Abdumotaleb El-Saddik, Tao Mei, Rita Cucchiara, Marco Bertini, Diana Patricia Tobon Vallejo, Pradeep K. Atrey, and M. Shamim Hossain (Eds.). ACM, 4848–4857. <https://doi.org/10.1145/3581783.3611698>
- [36] Qian Ning, Weisheng Dong, Xin Li, Jinjian Wu, and Guangming Shi. 2021. Uncertainty-driven loss for single image super-resolution. *Advances in Neural Information Processing Systems* 34 (2021), 16398–16409.
- [37] Rui Qin, Ming Sun, Fangyuan Zhang, Xing Wen, and Bin Wang. 2023. Blind Image Super-resolution with Rich Texture-Aware Codebook. In *Proceedings of the 31st ACM International Conference on Multimedia, MM 2023, Ottawa, ON, Canada, 29 October 2023- 3 November 2023*, Abdumotaleb El-Saddik, Tao Mei, Rita Cucchiara, Marco Bertini, Diana Patricia Tobon Vallejo, Pradeep K. Atrey, and M. Shamim Hossain (Eds.). ACM, 676–687. <https://doi.org/10.1145/3581783.3611917>
- [38] Robin Rombach, Andreas Blattmann, Dominik Lorenz, Patrick Esser, and Björn Ommer. 2021. High-Resolution Image Synthesis with Latent Diffusion Models. *arXiv:2112.10752* [cs.CV]
- [39] Wuxuan Shi, Mang Ye, and Bo Du. 2022. Symmetric Uncertainty-Aware Feature Transmission for Depth Super-Resolution. In *MM '22: The 30th ACM International Conference on Multimedia, Lisboa, Portugal, October 10 - 14, 2022*, João Magalhães, Alberto Del Bimbo, Shin'ichi Satoh, Nicu Sebe, Xavier Alameda-Pineda, Qin Jin, Vincent Oria, and Laura Toni (Eds.). ACM, 3867–3876. <https://doi.org/10.1145/3503161.3547873>
- [40] Liangchen Song, Jialian Wu, Ming Yang, Qian Zhang, Yuan Li, and Junsong Yuan. 2021. Handling Difficult Labels for Multi-label Image Classification via Uncertainty Distillation. In *MM '21: ACM Multimedia Conference, Virtual Event, China, October 20 - 24, 2021*, Heng Tao Shen, Yueting Zhuang, John R. Smith, Yang

929  
930  
931  
932  
933  
934  
935  
936  
937  
938  
939  
940  
941  
942  
943  
944  
945  
946  
947  
948  
949  
950  
951  
952  
953  
954  
955  
956  
957  
958  
959  
960  
961  
962  
963  
964  
965  
966  
967  
968  
969  
970  
971  
972  
973  
974  
975  
976  
977  
978  
979  
980  
981  
982  
983  
984  
985  
986987  
988  
989  
990  
991  
992  
993  
994  
995  
996  
997  
998  
999  
1000  
1001  
1002  
1003  
1004  
1005  
1006  
1007  
1008  
1009  
1010  
1011  
1012  
1013  
1014  
1015  
1016  
1017  
1018  
1019  
1020  
1021  
1022  
1023  
1024  
1025  
1026  
1027  
1028  
1029  
1030  
1031  
1032  
1033  
1034  
1035  
1036  
1037  
1038  
1039  
1040  
1041  
1042  
1043  
1044

- 1045 Yang, Pablo César, Florian Metze, and Balakrishnan Prabhakaran (Eds.). ACM, 2410–2419. <https://doi.org/10.1145/3474085.3475406>
- 1046 [41] Yukun Su, Guosheng Lin, Ruizhou Sun, Yun Hao, and Qingyao Wu. 2021. Modeling the Uncertainty for Self-supervised 3D Skeleton Action Representation Learning. In *MM '21: ACM Multimedia Conference, Virtual Event, China, October 20 - 24, 2021*, Heng Tao Shen, Yueting Zhuang, John R. Smith, Yang Yang, Pablo César, Florian Metze, and Balakrishnan Prabhakaran (Eds.). ACM, 769–778. <https://doi.org/10.1145/3474085.3475248>
- 1048 [42] Haoze Sun, Wenbo Li, Jianzhuang Liu, Haoyu Chen, Renjing Pei, Xueyi Zou, Youliang Yan, and Yujiu Yang. 2023. CoSeR: Bridging Image and Language for Cognitive Super-Resolution. *arXiv preprint arXiv:2311.16512* (2023).
- 1049 [43] Philippe Thévenaz, Thierry Blu, and Michael Unser. 2000. *Image Interpolation and Resampling*. 393–420. <https://doi.org/10.1016/b978-012077790-7/50030-8>
- 1050 [44] Boyang Wang, Yan Wang, Qing Zhao, Junxiang Lin, Zeng Tao, Pinxue Guo, Zhaoyu Chen, Kaixun Jiang, Shaoqi Yan, Shuyong Gao, and Wenqiang Zhang. 2023. A Capture to Registration Framework for Realistic Image Super-Resolution in the Industry Environment. In *Proceedings of the 31st ACM International Conference on Multimedia, MM 2023, Ottawa, ON, Canada, 29 October 2023- 3 November 2023*, Abdulmoteleb El-Saddik, Tao Mei, Rita Cucchiara, Marco Bertini, Diana Patricia Tobon Vallejo, Pradeep K. Atrey, and M. Shamim Hossain (Eds.). ACM, 7403–7412. <https://doi.org/10.1145/3581783.3611973>
- 1051 [45] Jianyi Wang, Zongsheng Yue, Shangchen Zhou, Kelvin CK Chan, and Chen Change Loy. 2023. Exploiting Diffusion Prior for Real-World Image Super-Resolution. In *arXiv preprint arXiv:2305.07015*.
- 1052 [46] Kai Wang, Xiaojiang Peng, Jianfei Yang, Shijian Lu, and Yu Qiao. 2020. Suppressing uncertainties for large-scale facial expression recognition. In *Proceedings of the IEEE/CVF conference on computer vision and pattern recognition*. 6897–6906.
- 1053 [47] Longguang Wang, Yingqian Wang, Xiaoyu Dong, Qingyu Xu, Jungang Yang, Wei An, and Yulan Guo. 2021. Unsupervised Degradation Representation Learning for Blind Super-Resolution. In *2021 IEEE/CVF Conference on Computer Vision and Pattern Recognition (CVPR)*. IEEE.
- 1054 [48] Xintao Wang, Liangbin Xie, Chao Dong, and Ying Shan. 2021. Real-esrgan: Training real-world blind super-resolution with pure synthetic data. In *Proceedings of the IEEE/CVF international conference on computer vision*. 1905–1914.
- 1055 [49] Yanbo Wang, Shaohui Lin, Yanyun Qu, Haiyan Wu, Zhizhong Zhang, Yuan Xie, and Angela Yao. 2021. Towards compact single image super-resolution via contrastive self-distillation. *arXiv preprint arXiv:2105.11683* (2021).
- 1056 [50] Yinhuai Wang, Jiwen Yu, and Jian Zhang. 2023. Zero-Shot Image Restoration Using Denoising Diffusion Null-Space Model. *The Eleventh International Conference on Learning Representations* (2023).
- 1057 [51] Pengxu Wei, Ziwei Xie, Hannan Lu, Zongyuan Zhan, Qixiang Ye, Wangmeng Zuo, and Liang Lin. 2020. Component divide-and-conquer for real-world image super-resolution. In *Computer Vision—ECCV 2020: 16th European Conference, Glasgow, UK, August 23–28, 2020, Proceedings, Part VIII 16*. Springer, 101–117.
- 1058 [52] Bin Xia, Yapeng Tian, Yulun Zhang, Yucheng Hang, Wenming Yang, and Qingmin Liao. 2023. Meta-learning based degradation representation for blind super-resolution. *IEEE Transactions on Image Processing* (2023).
- 1059 [53] Bin Xia, Yulun Zhang, Yitong Wang, Yapeng Tian, Wenming Yang, Radu Timofte, and Luc Van Gool. 2022. Knowledge distillation based degradation estimation for blind super-resolution. *arXiv preprint arXiv:2211.16928* (2022).
- 1060 [54] Yulong Xu, Sheng-Tsaing Tseng, Yu Tseng, Hsien-Kai Kuo, and Yi-Min Tsai. 2020. Unified Dynamic Convolutional Network for Super-Resolution with Variational Degradations. (Apr 2020).
- 1061 [55] Chenyu Yang, Mengxi Chen, Yanfeng Wang, and Yu Wang. 2023. Uncertainty-Guided End-to-End Audio-Visual Speaker Diarization for Far-Field Recordings. In *Proceedings of the 31st ACM International Conference on Multimedia, MM 2023, Ottawa, ON, Canada, 29 October 2023- 3 November 2023*, Abdulmoteleb El-Saddik, Tao Mei, Rita Cucchiara, Marco Bertini, Diana Patricia Tobon Vallejo, Pradeep K. Atrey, and M. Shamim Hossain (Eds.). ACM, 4031–4041. <https://doi.org/10.1145/3581783.3612424>
- 1062 [56] Jianchao Yang, John Wright, Thomas S Huang, and Yi Ma. 2010. Image Super-Resolution Via Sparse Representation. *IEEE Transactions on Image Processing* (Nov 2010), 2861–2873. <https://doi.org/10.1109/tip.2010.2050625>
- 1063 [57] Zexian Yang, Dayan Wu, Wanqian Zhang, Bo Li, and Weiping Wang. 2023. Handling Label Uncertainty for Camera Incremental Person Re-Identification. In *Proceedings of the 31st ACM International Conference on Multimedia, MM 2023, Ottawa, ON, Canada, 29 October 2023- 3 November 2023*, Abdulmoteleb El-Saddik, Tao Mei, Rita Cucchiara, Marco Bertini, Diana Patricia Tobon Vallejo, Pradeep K. Atrey, and M. Shamim Hossain (Eds.). ACM, 6253–6263. <https://doi.org/10.1145/3581783.3612294>
- 1064 [58] Fuming You, Jingjing Li, Zhi Chen, and Lei Zhu. 2022. Pixel Exclusion: Uncertainty-aware Boundary Discovery for Active Cross-Domain Semantic Segmentation. In *MM '22: The 30th ACM International Conference on Multimedia, Lisboa, Portugal, October 10 - 14, 2022*, João Magalhães, Alberto Del Bimbo, Shin'ichi Satoh, Nicu Sebe, Xavier Alameda-Pineda, Qin Jin, Vincent Oria, and Laura Toni (Eds.). ACM, 1866–1874. <https://doi.org/10.1145/3503161.3548079>
- 1065 [59] Zongsheng Yue, Jianyi Wang, and Chen Change Loy. 2024. Resshift: Efficient diffusion model for image super-resolution by residual shifting. *Advances in Neural Information Processing Systems* 36 (2024).
- 1066 [60] Zongsheng Yue, Qian Zhao, Jianwen Xie, Lei Zhang, Deyu Meng, and Kwan-Yee K Wong. 2022. Blind image super-resolution with elaborate degradation modeling on noise and kernel. In *Proceedings of the IEEE/CVF conference on computer vision and pattern recognition*. 2128–2138.
- 1067 [61] Syed Waqas Zamir, Aditya Arora, Salman Khan, Munawar Hayat, Fahad Shahbaz Khan, and Ming-Hsuan Yang. 2022. Restormer: Efficient Transformer for High-Resolution Image Restoration. In *CVPR*.
- 1068 [62] Jinlu Zhang, Yujin Chen, and Zhiqiang Tu. 2022. Uncertainty-Aware 3D Human Pose Estimation from Monocular Video. In *MM '22: The 30th ACM International Conference on Multimedia, Lisboa, Portugal, October 10 - 14, 2022*, João Magalhães, Alberto Del Bimbo, Shin'ichi Satoh, Nicu Sebe, Xavier Alameda-Pineda, Qin Jin, Vincent Oria, and Laura Toni (Eds.). ACM, 5102–5113. <https://doi.org/10.1145/3503161.3547773>
- 1069 [63] Kai Zhang, Jingyun Liang, Luc Van Gool, and Radu Timofte. 2021. Designing a practical degradation model for deep blind image super-resolution. In *Proceedings of the IEEE/CVF International Conference on Computer Vision*. 4791–4800.
- 1070 [64] Wenyu Zhang, Xin Deng, Baojun Jia, Xingtong Yu, Yifan Chen, Jin Ma, Qing Ding, and Xinming Zhang. 2023. Pixel Adapter: A Graph-Based Post-Processing Approach for Scene Text Image Super-Resolution. In *Proceedings of the 31st ACM International Conference on Multimedia, MM 2023, Ottawa, ON, Canada, 29 October 2023- 3 November 2023*, Abdulmoteleb El-Saddik, Tao Mei, Rita Cucchiara, Marco Bertini, Diana Patricia Tobon Vallejo, Pradeep K. Atrey, and M. Shamim Hossain (Eds.). ACM, 2168–2179. <https://doi.org/10.1145/3581783.3611913>
- 1071 [65] Yong Zhao, Haifeng Chen, Hichem Sahli, Ke Lu, and Dongmei Jiang. 2022. Uncertainty-Aware Semi-Supervised Learning of 3D Face Rigging from Single Image. In *MM '22: The 30th ACM International Conference on Multimedia, Lisboa, Portugal, October 10 - 14, 2022*, João Magalhães, Alberto Del Bimbo, Shin'ichi Satoh, Nicu Sebe, Xavier Alameda-Pineda, Qin Jin, Vincent Oria, and Laura Toni (Eds.). ACM, 170–179. <https://doi.org/10.1145/3503161.3548285>
- 1072 [66] Hongyang Zhou, Xiaobin Zhu, Jianqing Zhu, Zheng Han, Shi-Xue Zhang, Jingyan Qin, and Xu-Cheng Yin. 2023. Learning Correction Filter via Degradation-Adaptive Regression for Blind Single Image Super-Resolution. In *Proceedings of the IEEE/CVF International Conference on Computer Vision*. 12365–12375.
- 1073 [67] Linyi Zhou, Xijian Fan, Yingjie Ma, Tardi Tjahjadi, and Qiaolin Ye. 2020. Uncertainty-aware Cross-dataset Facial Expression Recognition via Regularized Conditional Alignment. In *MM '20: The 28th ACM International Conference on Multimedia, Virtual Event / Seattle, WA, USA, October 12-16, 2020*, Chang Wen Chen, Rita Cucchiara, Xian-Sheng Hua, Guo-Jun Qi, Elisa Ricci, Zhengyou Zhang, and Roger Zimmermann (Eds.). ACM, 2964–2972. <https://doi.org/10.1145/3394171.3413515>
- 1074 [68] Zhou Zhou, Jiahao Chao, Jiali Gong, Hongfan Gao, Zhenbing Zeng, and Zhengfeng Yang. 2023. Enhancing Real-Time Super Resolution with Partial Convolution and Efficient Variance Attention. In *Proceedings of the 31st ACM International Conference on Multimedia, MM 2023, Ottawa, ON, Canada, 29 October 2023- 3 November 2023*, Abdulmoteleb El-Saddik, Tao Mei, Rita Cucchiara, Marco Bertini, Diana Patricia Tobon Vallejo, Pradeep K. Atrey, and M. Shamim Hossain (Eds.). ACM, 5348–5357. <https://doi.org/10.1145/3581783.3611729>
- 1075 1103
- 1076 1104
- 1077 1105
- 1078 1106
- 1079 1107
- 1080 1108
- 1081 1109
- 1082 1110
- 1083 1111
- 1084 1112
- 1085 1113
- 1086 1114
- 1087 1115
- 1088 1116
- 1089 1117
- 1090 1118
- 1091 1119
- 1092 1120
- 1093 1121
- 1094 1122
- 1095 1123
- 1096 1124
- 1097 1125
- 1098 1126
- 1099 1127
- 1100 1128
- 1101 1129
- 1102 1130
- 1131
- 1132
- 1133
- 1134
- 1135
- 1136
- 1137
- 1138
- 1139
- 1140
- 1141
- 1142
- 1143
- 1144
- 1145
- 1146
- 1147
- 1148
- 1149
- 1150
- 1151
- 1152
- 1153
- 1154
- 1155
- 1156
- 1157
- 1158
- 1159
- 1160